

## Double-Crystal Spectrometer Measurements of Lattice Parameters and X-ray Topography on Heterojunctions GaAs-Al<sub>x</sub>Ga<sub>1-x</sub>As

By E. ESTOP\*, A. IZRAEL AND M. SAUVAGE

*Laboratoire de Minéralogie-Cristallographie, associé au CNRS, Université P. et M. Curie, 4 place Jussieu, 75230 Paris Cedex 05, France*

(Received 2 December 1975; accepted 4 February 1976)

Heterojunctions GaAs-Al<sub>x</sub>Ga<sub>1-x</sub>As involved in the elaboration of IR laser diodes have been studied. The difference in lattice parameter between the GaAs substrate and the aluminum-substituted epitaxial layer Al<sub>x</sub>Ga<sub>1-x</sub>As has been measured accurately on a double-crystal spectrometer for a series of compositions. These data coupled with radius of curvature determination have permitted calculation of the stress in the layer and the bulk lattice parameter of Al<sub>x</sub>Ga<sub>1-x</sub>As. Characterization of the defects introduced during the liquid-phase epitaxy has been performed by X-ray topography.

### Introduction

The elaboration of multiple heterojunctions for infrared laser semiconductor devices involves as a first step the deposition of a layer of aluminum-substituted gallium arsenide Al<sub>x</sub>Ga<sub>1-x</sub>As on a gallium arsenide substrate by liquid-phase epitaxy (LPE). Since both crystals have different parameters at room temperature, the matching of the two lattices along the interface is not perfect and elastic strains or plastic deformation may occur in the sample. The presence of such defects significantly decreases the lifetime of the devices and numerous studies have been performed to improve the understanding of defect generation.

The purpose of the present work is to measure accurately the difference in lattice parameter between the epitaxial layer and the substrate and the resulting curvature of the sample. Such measurements have already been performed by Rozgonyi, Petroff & Panish (1974) and Druzhinina *et al.* (1975). However the results obtained by the two groups were contradictory and it was thought worthwhile to make additional experiments. Actually, the results of the present work show that the disagreement between previous data is only apparent and is due to a lack of detailed analysis.

### Sample characteristics

The samples were provided by the C.G.E. Research Laboratories who performed the liquid-phase epitaxy on Monsanto Laboratory gallium arsenide substrates heavily doped with silicon (more than 10<sup>18</sup> atoms per cm<sup>3</sup>). The epitaxy was followed by accurate measurements of the layer thickness and composition. Although the microprobe analysis is subject to many uncertainties, one can be rather confident in the assigned composition values since they have been controlled by an independent technique, namely the measurement of the energy gap in Al<sub>x</sub>Ga<sub>1-x</sub>As as a function

\* Present address: Facultad de Ciencias, Departamento de Cristalografía y Mineralogía, Avda. J. Antonio 585, Barcelona 7, Spain.

of  $x$  by Barbé (1974). The accuracy in composition of the epilayer is then better than a few percent. Prior to epitaxy, the samples had been etched in a mixture H<sub>2</sub>SO<sub>4</sub>-H<sub>2</sub>O<sub>2</sub>-H<sub>2</sub>O (4:1:1). The investigated crystals are rectangular (100) wafers (6 × 12 × 0.25 mm) with cleaved edges along [011] and [01 $\bar{1}$ ]. The epitaxial layer is a few  $\mu\text{m}$  thick (see Table 1a) and as a result of the deposition technique, the concentration in Al decreases from the interface to the external surface at a rate of 0.5%  $\mu\text{m}^{-1}$  (Barbé, 1974).

Table 1. *Experimental data*

(a) Measured  $K\alpha_1$  peak shift ( $''$ ), radius of curvature of the wafer  $\rho$  (m) and average stress in the epilayer  $\sigma_1$  ( $\times 10^8$  dyn cm<sup>-2</sup>) as functions of aluminum content  $x$  and layer thickness  $t_1$  ( $\mu\text{m}$ ).

$x$	$t_1$	$\Delta\theta_x$	$\rho$	$\sigma_1$
0	2.30	0	$\infty$	0
0.12	3.66	44	15.8	2.26
0.24	4.15	82	6.8	4.64
0.39	3.66	144	3.9	9.2
0.54	3.05	204	4.0	10.7
0.68	2.80	236	4.0	11.7
0.79	2.44	285	3.3	16.3

(b) Relative parameter difference between layer and substrate in the strained state ( $\Delta a_s^1/a_s$ ) ( $\times 10^{-4}$ ), strains in the layer  $\Delta a_l/a$  ( $\times 10^{-4}$ ) and substrate  $\Delta a_s/a$  ( $\times 10^{-5}$ ), relative parameter difference in the strain-free state ( $\Delta a_s^0/a_s$ ) ( $\times 10^{-4}$ ) as functions of  $x$ .

$x$	$\left(\frac{\Delta a_s^1}{a}\right)_0$	$\frac{\Delta a_l}{a}$	$\frac{\Delta a_s}{a}$	$\left(\frac{\Delta a_s^0}{a}\right)_0$
0	0	0	0	0
0.12	3.28	1.36	0.79	1.84 ± 0.25
0.24	6.12	2.78	1.85	3.16 ± 0.35
0.39	10.7	5.52	3.23	4.86 ± 0.55
0.54	15.2	6.42	3.13	8.47 ± 0.62
0.68	17.6	7.02	3.14	10.27 ± 0.66
0.79	21.3	9.78	3.80	11.14 ± 0.86
1	Debye-Scherrer measurement			14.8 ± 2.5

### Experimental techniques

(a) *Measurement of the parameter of Al<sub>x</sub>Ga<sub>1-x</sub>As*

A double-crystal spectrometer was used to measure the shift  $\Delta\theta_x$  of the  $K\alpha_1$  reflexion peak between the

GaAs substrate and the epitaxial layer  $\text{Al}_x\text{Ga}_{1-x}\text{As}$ . The first crystal is a perfect GaAs single crystal adjusted for the 400 reflexion of  $\text{Cu } K\alpha_1$  in the symmetrical Laue case (transmission setting). In order to prevent the simultaneous reflexion of  $\text{Cu } K\alpha_2$ , a  $\frac{1}{30}^\circ$  divergence slit is inserted before the first crystal. The sample under investigation is taken as second crystal and adjusted in the symmetrical Bragg case (reflection setting). It has been checked that when the sample is flat or only slightly curved, the full width at half maximum (FWHM) of the rocking curve is close to the theoretical value of  $8.5''$  but that it increases with increasing curvature (see Fig. 1). With such narrow profiles, there is no peak overlap as was the case in the experimental determination by Rozgonyi *et al.* (1974) and the value of the  $K\alpha_1$  peak shift  $\Delta\theta_x$  is obtained with an absolute error of  $\pm 2''$ . Since the corresponding value  $(\Delta a/a)_x$  of the measured relative lattice parameter variation is given by

$$\left(\frac{\Delta a}{a}\right)_x = \Delta\theta_x \cotan \theta \quad (1)$$

the absolute error on  $(\Delta a/a)_x$  is about  $\pm 1.5 \times 10^{-5}$ .

The measured peak shifts have been corrected for a possible pure rotation component.

#### (b) Direct measurement of the parameter of pure AlAs

Very pure AlAs (Cerac/Pure inc. 99.999%) was used for powder measurements on a 19 cm diameter Debye-Scherrer camera. Since the fine-grained powder is rapidly destroyed in air the samples were ground and loaded in capillary quartz tubes under a nitrogen atmosphere.

#### (c) Evaluation of the radius of curvature

The measurements were performed on a classical X-ray topography setting, the divergence of the incident beam being of the order of one minute of arc. The method, although manually controlled, is equivalent to the ABAC technique (automatic Bragg-angle control) described by Rozgonyi *et al.* (1974). The sample is moved in steps of 1.5 mm, each step being measured with an accuracy of  $10 \mu\text{m}$ . The FWHM of the reflexion profile is about  $60''$  and since the peak position can be located within  $\pm 5''$ , the error on the peak shift between two positions on the samples is  $\pm 10''$ . As a consequence, the homogeneity of the curvature is controlled within 20% whilst the curvature itself is measured with an accuracy of 10% making use of the largest interval, 4.5 mm. The exact geometry of the curvature has been analysed with the help of four different reflexions: 022, 02 $\bar{2}$ , 040, 004.

#### (d) Characterization of crystal perfection

Transmission X-ray topography was used prior to epitaxy to image the defects in the substrate. After epitaxy, the newly created defects were observed by both reflexion and transmission topography.

## Results and discussion

### (a) Lattice parameter of $\text{Al}_x\text{Ga}_{1-x}\text{As}$ as a function of $x$

Since the samples are curved, the measurements of the  $K\alpha_1$  peak shift  $\Delta\theta_x$  between the layer and substrate (Fig. 1) give the value of the relative parameter difference  $(\Delta a'_s/a)_s$  when both the epilayer and the substrate are in a strained state. If  $\Delta a_l/a$  and  $\Delta a_s/a$  represent the strains normal to the reflecting plane in the layer and substrate respectively, one has the following relation:

$$\left(\frac{\Delta a'_s}{a}\right)_s = \frac{\Delta a_l}{a} + \left(\frac{\Delta a'_s}{a}\right)_0 - \frac{\Delta a_s}{a} \quad (2)$$

Hence, in order to reach the corresponding  $(\Delta a'_s/a)_0$  for strain-free materials, it is necessary to determine the mean value of the stresses within a depth equivalent to the penetration distance of the X-ray beam. In the present case of the 400 reflexion with  $\text{Cu } K\alpha_1$  this distance is of the order of  $3 \mu\text{m}$ .

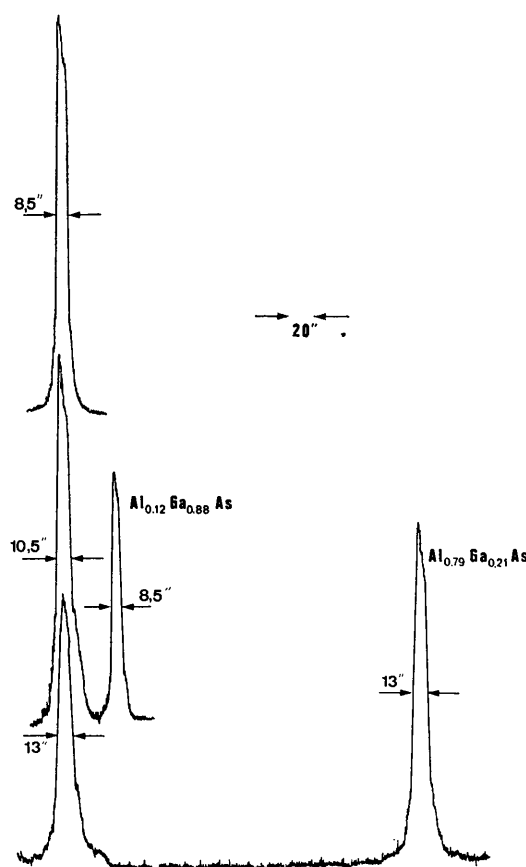


Fig. 1. 400 reflexion profiles recorded on a double spectrograph in the parallel setting with  $\text{Cu } K\alpha_1$  radiation. Upper curve: superimposed profiles of the GaAs substrate and epilayer; mid curve: shifted profiles of the substrate (left) and the  $\text{Al}_x\text{Ga}_{1-x}\text{As}$  epilayer (right) for  $x=0.12$ ; lower curve: shifted profiles for  $x=0.79$ .

It can be shown (Reinhart & Logan, 1973; Rozgonyi & Ciesielka, 1973) that when the thickness  $t_l$  of the epilayer is negligible with respect to the thickness  $t_s$  of the substrate, the expression for the average stress  $\sigma_l$  in the epilayer takes the form

$$\sigma_l = \frac{-E}{6\rho(1-\nu)} \frac{t_s^2}{t_l} \quad (3)$$

where  $E$  is Young's modulus ( $E=10^{12}$  dyne/cm<sup>2</sup>),  $\nu$  is Poisson's ratio ( $\nu=0.3$ ) and  $\rho$  is the radius of curvature of the sample.

In the same approximation the stress  $\sigma_s$  in the first  $\mu\text{m}$  of the substrate close to the interface is given by

$$\sigma_s = -4 \frac{t_l}{t_s} \sigma_l. \quad (4)$$

Then the strains can be readily calculated through the elasticity relation

$$\frac{\Delta a_{l(s)}}{a} = - \frac{2\nu}{E} \sigma_{l(s)}, \quad (5)$$

$\sigma_{l(s)}$  being determined by the measurement of the radius of curvature  $\rho$  described in the previous section. In the whole course of these calculations, the elastic constants of the layer and substrate are assumed to be equal; the validity of this assumption will be discussed later.

The experimental data  $\rho$ ,  $\Delta\theta_x$  and  $(\Delta a_s^l/a)_s$  are listed in Table 1 together with the calculated values of the stresses and strains; the resulting strain-free relative parameter differences  $(\Delta a_s^l/a)_0$  are listed in the last column for a series of samples with increasing Al content in the epilayer. It is worth noticing that in the first sample concerning the homoepitaxy of pure GaAs on a heavily doped GaAs substrate, the radius

of curvature was found to be infinite and no  $K\alpha_1$  peak shift could be detected.

The variation of  $(\Delta a_s^l/a)_0$  as a function of  $x$ , plotted in Fig. 2 is quite consistent with the linear behaviour predicted by Vegard's law, a result already obtained by Rozgonyi *et al.* (1974). The non-physical case of  $x=1$  (epitaxy of pure AlAs on GaAs) has been calculated on the basis of the present Debye-Scherrer measurements\* of the lattice parameters of pure GaAs and AlAs powders:  $a(\text{AlAs})=5.6612 \pm 0.0008$ ,  $a(\text{GaAs})=5.6528 \pm 0.0006$  Å.

A rough check of the consistency of the method is obtained by comparing the measured radius of curvature  $\rho$  with the value calculated on the basis of the relative parameter differences  $(\Delta a_s^l/a)_0$  listed in Table 1(b) according to the formula given by Reinhart *et al.* (1973):

$$\rho = \frac{C}{\left(\frac{\Delta a_s^l}{a}\right)_0} \frac{t_s^2}{6t_l}, \quad (6)$$

which is only valid if  $t_l$  is much smaller than  $t_s$  and where  $C$  denotes a function of the elastic constants of both compounds equal to one when these constants are assumed to be identical. In Table 2 the values calculated in the hypothesis  $C=1$  together with the best fit obtained by least-squares analysis and corresponding to  $C=0.93$  are compared with the experimental data. The comparison is rather satisfactory since the curvature was not perfectly homogenous although spherical, as was demonstrated by use of four different reflexions.

Table 2. Comparison between measured and calculated radius of curvature ( $\rho$ ) as a function of  $x$

$x$	$\rho$ measured	$\rho$ calculated with $C=1$	$\rho$ calculated with $C=0.93$
0.12	15.8	15.5	14.4
0.24	6.8	7.9	7.3
0.39	3.9	5.8	5.4
0.54	4.0	4.0	3.7
0.68	4.0	3.6	3.4
0.79	3.3	3.8	3.5

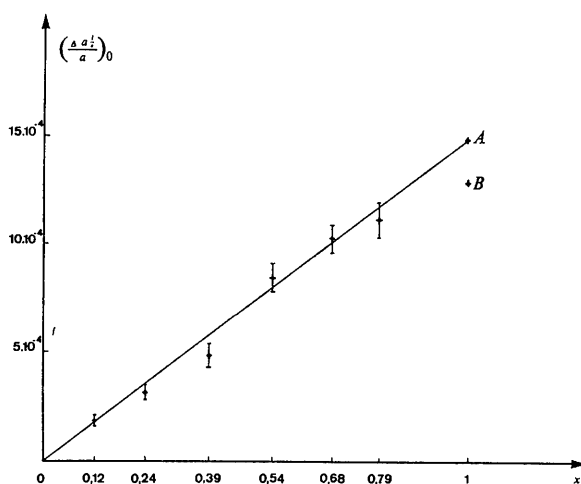


Fig. 2. Measured relative lattice parameter difference between GaAs and a strain-free solid solution  $\text{Al}_x\text{Ga}_{1-x}\text{As}$  as a function of  $x$ . Debye-Scherrer data for  $x=1$ : A present determination; B results of Ettenberg & Paff (1970); the solid line represents the prediction of Vegard's law.

It should be noticed that the results found in the present work agree with the data previously published independently by Rozgonyi *et al.* (1974) and by Druzhinina *et al.* (1975), although the two papers appear contradictory at first sight. The reason might be that Rozgonyi *et al.* produce relative parameter differences presumably corrected for strain contributions while Druzhinina *et al.* publish the  $(\Delta a_s^l/a)_s$  in the strained state as measured directly by the  $K\alpha_1$  peak shift.

\* The powder diagrams were taken by B. Künzler at the Laboratoire de Cristallographie aux Rayons X, University of Geneva.

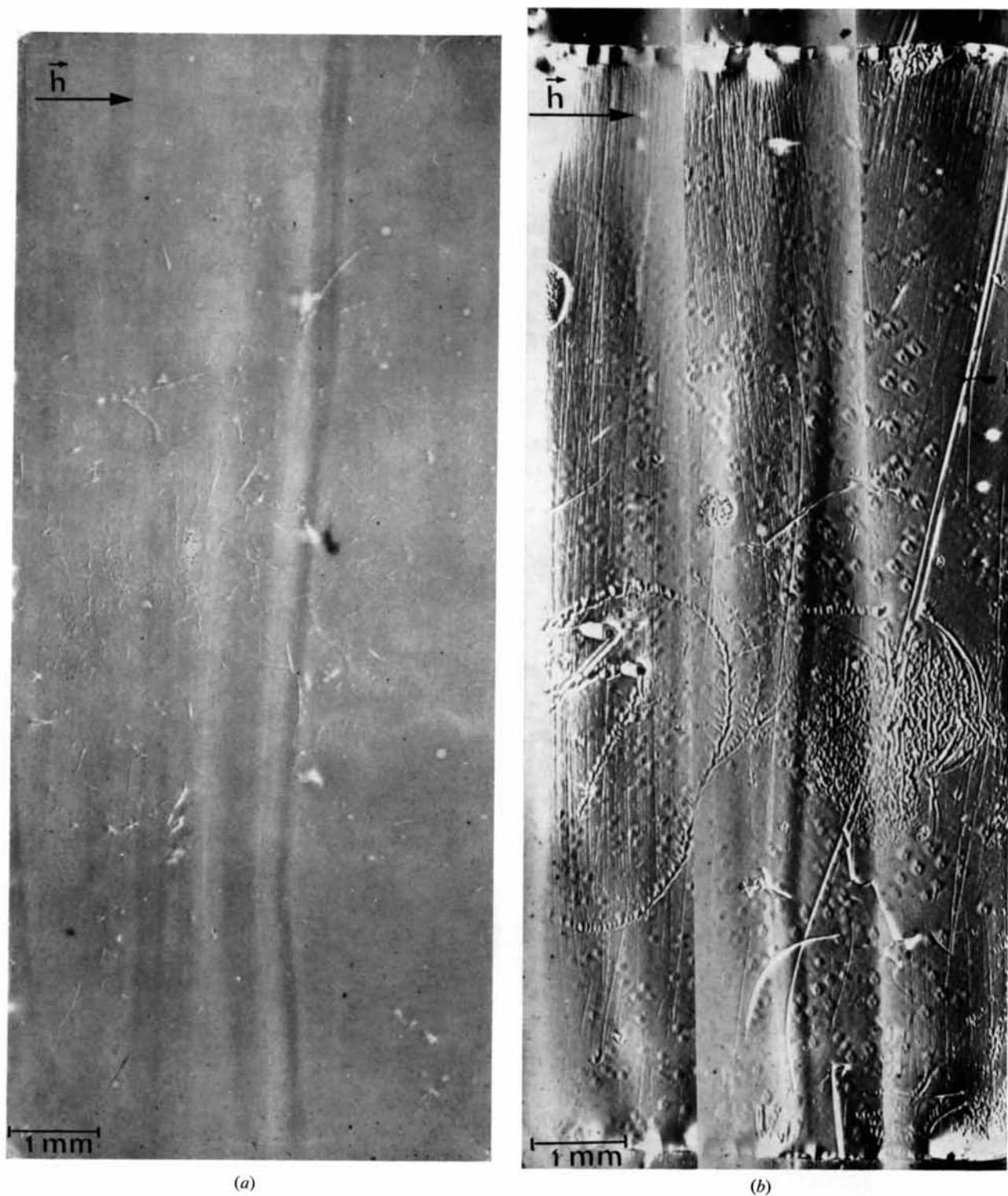


Fig. 3. Transmission topograph,  $02\bar{2}$  reflexion,  $\text{Mo } K\alpha_1$ . (a) Dislocation-free crystal prior to epitaxy, (b) same crystal after epitaxy of a  $4 \mu\text{m}$  thick layer of  $\text{Al}_x\text{Ga}_{1-x}\text{As}$  with  $x=0.3$ . Notice the newly created linear defects.

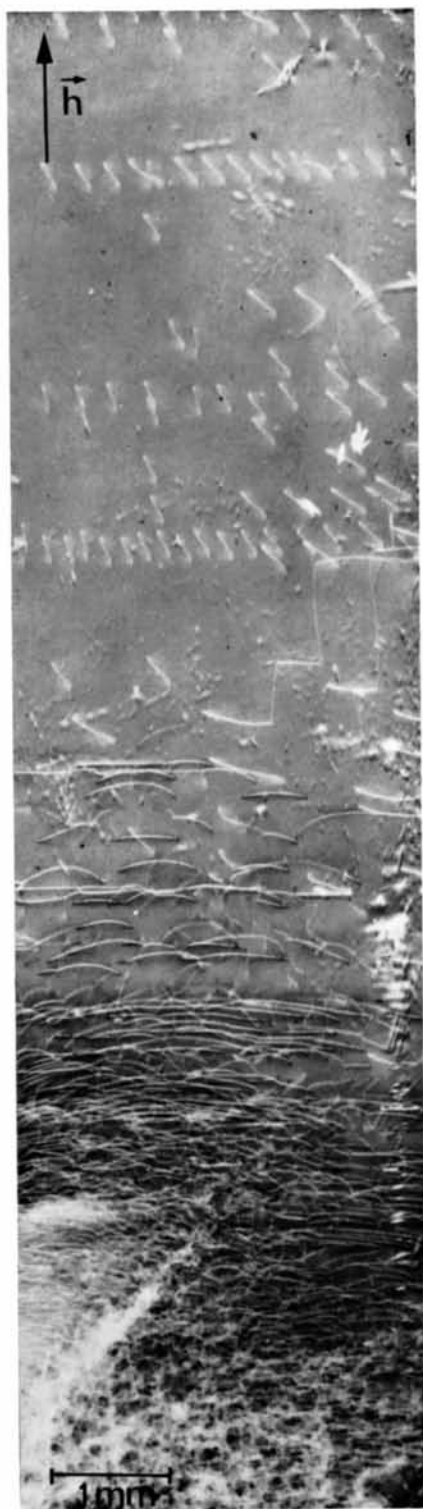
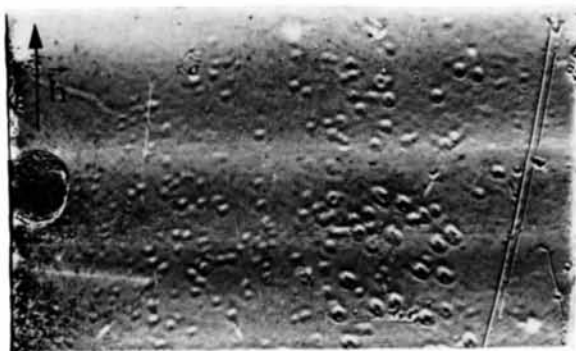


Fig. 4. Borrmann transmission topograph, 022 reflexion, Mo  $K\alpha_1$ , GaAs substrate showing a large variety of dislocations.



(a)



(b)



(c)

Fig. 5. Misfit dislocations. (a) Reflexion topograph, 402 reflexion on the epitaxial layer only, Cu  $K\alpha_1$ , the dislocations are visible, (b) transmission topograph, Mo  $K\alpha_1$ , 022 reflexion, (c) reflexion topograph, Cu  $K\alpha_1$ , 444 reflexion on the epitaxial layer. The dislocations are out of contrast in (b) and (c).

Making use of formulae (3), (4), (5) and (6) it is possible to express the strain components in terms of the strain-free value  $(\Delta a_s^t/a)_0$ . Hence, expression (2) takes the form:

$$\left(\frac{\Delta a_s^t}{a}\right)_s = \left(1 + \frac{2\nu}{1-\nu} + \frac{8\nu}{1-\nu} \times \frac{t_l}{t_s}\right) \left(\frac{\Delta a_s^t}{a}\right)_0 \quad (7)$$

Since in the cases of interest here,  $t_l/t_s$  lies between  $10^{-2}$  and  $1.6 \times 10^{-2}$ , formula (7) leads to

$$\left(\frac{\Delta a_s^t}{a}\right)_s = 1.9 \left(\frac{\Delta a_s^t}{a}\right)_0 \quad (8)$$

This simple result explains why the measured value related to the  $K\alpha_1$  peak shift is about twice as large as the value given by Vegard's law. On this point it can be summarized that the present measurements agree with Druzhinina *et al.* (1975) and lead to corrected values confirming those of Rozgonyi *et al.* (1974).

### (b) Defects related with liquid-phase epitaxy

As was developed in the previous section, GaAs and  $\text{Al}_x\text{Ga}_{1-x}\text{As}$  have different lattice parameters at room temperature. However, because of the difference in thermal expansion coefficients, the mismatch vanishes for any value of  $x$  around  $900^\circ\text{C}$ , which is near to the temperature chosen for the LPE ( $845^\circ\text{C}$ ) (Ettenberg & Paff, 1970; Pierron, Parker & McNeely, 1966). This property was corroborated by following the progressive overlap of the reflexion peaks from the layer and substrate on increasing the temperature from  $25$  to  $850^\circ\text{C}$  (Barrault, 1975). The epitaxial layer thus grows strain free, but stresses appear on cooling resulting in the elastic spherical curvature of the sample already described in this paper. However, if the threshold for misfit dislocation generation is surpassed, some dislocations may appear in the interface between layer and substrate. In order to have more information on this phenomenon, X-ray topographs of the same sample were taken before and after LPE. Most substrates show no grown-in dislocations but only broad bands due to an irregular dopant distribution (Fig. 3a). In some samples dislocation pile-up in  $\{111\}$  glide planes, or more complicated dislocation tangles presumably introduced during handling or cleaving, were observed (Fig. 4). It should be noticed that in such a highly absorbant sample ( $\mu t = 8.7$ ) the contrast is purely dynamical and dislocations appear as white lines on a dark grey background.

After epitaxy, newly created linear defects parallel to the  $[011]$  direction are sometimes observed as is shown in a transmission topograph (Fig. 3b)\* and in a reflexion topograph as well (Fig. 5a). In the transmission setting, the major contribution to the image comes

from the substrate since the rays belonging to the reflexion domain of the epilayer have been absorbed out before reaching it. As a consequence, the presence in Fig. 3(b) of white dynamical images of the linear dislocations provides evidence for their belonging to the substrate. On the other hand, Fig. 5(a) represents a reflexion topograph taken with the 402 reflexion. Since such reflexions ( $h+k+l \neq 4n$ ) have a vanishingly small structure factor in GaAs one can be sure that the topograph is only due to the epilayer  $\text{Al}_{0.3}\text{Ga}_{0.7}\text{As}$ . Hence the presence of the linear dislocations in Fig. 5(a) indicates that they belong also to the epilayer and are thus located in the interface. The dislocations are pure edge with Burgers vector  $\frac{1}{2}[01\bar{1}]$ , as can be seen from Fig. 5(b) and (c) where they are out of contrast. They are most likely misfit dislocations generated on local stress concentrations, but their density is far too low to accommodate the lattice mismatch which is properly accounted for by the curvature.

### Conclusion

The present measurements have permitted elucidation of the misunderstandings between independent groups working in the field of heterojunctions on GaAs. The results provide confirmation of the order of magnitude of the stresses in the epitaxial layers and establish the compatibility of the parameter variation in stress-free  $\text{Al}_x\text{Ga}_{1-x}\text{As}$  with the prediction of Vegard's law. Further work on multiple heterojunctions with phosphorus addition is in progress.

The authors are greatly indebted towards J. Benoit and his co-workers from the C.G.E. research laboratories who provided them with the samples and performed all the measurements on the epitaxial layer characteristics. One of us (E.E.) wishes to thank the French government for a CROUS research grant. This work has been partly supported by a contract with the DGRST (No. 74.7.0420).

### References

- BARBÉ, M. (1974). Thèse de 3ème cycle, Paris (unpublished).  
 BARRAULT, J. V. (1975). Private communication.  
 DRUZHININA, L. V., BUBLIK, V. T., DOLGINOV, L. M., ELISEEV, P. G., KERBELEV, M. P., OSVENSII, V. B., PINSKER, I. Z. & SHUMSKII, M. G. (1975). *Sov. Phys. Tech. Phys.* **7**, 935-939.  
 ETTEMBERG, M. & PAFF, R. J. (1970). *J. Appl. Phys.* **41**, 3926-3927.  
 PIERRON, E. D., PARKER, D. L. & MCNEELY, J. B. (1966). *Acta Cryst.* **21**, 290.  
 REINHARDT, F. K. & LOGAN, R. A. (1973). *J. Appl. Phys.* **44**, 3171-3175.  
 ROZGONYI, G. A. & CIESIELKA, T. J. (1973). *Rev. Sci. Instrum.* **44**, 1053-1057.  
 ROZGONYI, G. A., PETROFF, P. M. & PANISH, M. B. (1974). *J. Cryst. Growth.* **27**, 106-117.  
 SMALL, M. B., BLAKESLEE, A. E., SHIH, K. K. & POTEMSKI, R. M. (1975). *J. Cryst. Growth*, **30**, 257-266.

\* Morphological surface defects due to gallium droplets (Small *et al.*, 1975) are also visible on this topograph, such defects are now eliminated by a better control of the growth process.